SBGf09899

Ray tracing by simulated annealing in complicated 3-D models

Danilo R. Velis and Tadeusz J. Ulrych

University of British Columbia

Abstract

We present a novel ray-tracing method for obtaining the minimum traveltime raypath connecting any two fixed points in complicated 3-D geological models. The problem is cast as a nonlinear optimization problem where the cost function (traveltime) is globally minimized with respect to the take-off angles by means of simulated annealing (SA). As opposed to conventional ray tracing methods (e.g. shooting and bending), the new technique overcomes some well-known difficulties regarding multipathing and take-off angles selection, specially in complex 3-D structures. These include local convergence (i.e. failing to obtain the raypath with absolute minimum traveltime) and divergence of the take-off angle selection strategy. Under these circumstances, shooting and bending methods do not provide confidence on the results at a reasonable computational effort. We explore the behavior of the new method using a fault model and a salt-dome model. Also, we present a versatile model representation that can be used to accommodate a large class of geological models. The results demonstrate the ability of the new technique of solving the two-point ray-tracing problem in complex 3-D media accurately and efficiently.

INTRODUCTION

Several methods for solving the two-point ray-tracing problem in 3-D media have been developed in the literature (e.g. Červený, 1987; Moser et al., 1992). These are shooting and bending algorithms that proceed iteratively from an initial guess until the ray arrives to the receiver or the traveltime is stationary (Fermat's principle). When more than one raypath exists between source and receiver, usually these methods converge to the raypath that is closest to the initial guess.

In the shooting method, first an initial point (*source*) is fixed and a fan of rays is propagated by specifying a set of take-off angles. After selecting those angles that generate raypaths arriving to the receiver neighborhood, a search strategy is applied to update the angles until the ray emerges through the desired endpoint (*receiver*) within a given tolerance. Since frequently the receiver location is an ill-behaved function of the take-off angles, the search strategy may fail or show poor convergence, and as a consequence, some raypaths might be missed. Attempts to obtain the global minimum traveltime raypath for 2-D models have been made by Sambridge and Kennett (1990), but convergence to the global minimum is not guaranteed, specially in complicated 3-D structures.

In the bending method both end points are linked by an initial guess path, which is then perturbed iteratively so as to satisfy the ray equations or Fermat's principle of stationary time. Unlike shooting, bending always produces a ray connecting source and receiver. Since in general bending involves the solution of a nonlinear optimization problem, which requires some kind of gradient directions to update the raypath, it tends to overlook multipathing propagation because the solution depends on the first guess. Methods based on advanced graph theory for choosing an initial guess close to the global minimum exist (e.g. Fisher and Lees, 1993), but the implementation of these techniques in complex 3-D structures is limited not only because of computer memory issues, but also because the computation time increases dramatically when the node spacing, for accuracy purposes, is reduced.

Recently, Velis and Ulrych (1996) presented a new ray-tracing method, called *simulated annealing ray tracing* (SART), that overcomes the mentioned difficulties in 2-D models. Here SART is extended to 3-D models and further improvements concerning accuracy and efficiency are incorporated into the original scheme. Essentially, the two-point ray tracing problem is put into a nonlinear optimization framework which is in turn solved by means of *very fast simulated annealing* (VFSA) (Ingber, 1989). This guarantees convergence to the global minimum of the cost function that represents the total traveltime from source to receiver.

EARTH MODEL

The velocity model, which is contained within the cube $(x_{min}, x_{max}) \times (y_{min}, y_{max}) \times (z_{min}, z_{max})$, is composed of any number of regions separated by curved interfaces representing geologic horizons, fault planes, etc. We assume all interfaces are explicit functions of the form $z = g(x, y)$. The velocity within each region may be specified by any function $v = v(\mathbf{x})$, $\mathbf{x} = (x, y, z)$, and must be twice differentiable. Interfaces may or may not intercept each other, allowing for a greater

flexibility to construct a wide variety of models, including complex 3-D structures. Take Figure 1 as an example, where we constructed two blocky models: a fault model and a salt-dome model.

INITIAL-VALUE PROBLEM (IVP)

Like in shooting, given an initial point, $\mathbf{x}_s$, and an initial set of take-off angles, (θ_s, ξ_s), we solve the ray equations using Euler and Runge-Kutta methods. Here subscript s stands for *source*, and θ and ξ stand for declination and azimuth angles which describe the ray direction at every point of its trajectory.

Solving the IVP is not a trivial task. The ray propagates until it finds an interface. At this stage it is necessary to obtain the intersection point between the raypath and the interface, and to apply Snell's Law. Then the propagation resumes with the new initial conditions, until the ray endpoint arrives to a model boundary, where propagation stops. Also, the propagation stops when the ray arrives at a predefined target surface (usually a plane) passing through the receiver (e.g. a vertical plane in a borehole experiment). During the propagation, an index indicating the current region the ray is traversing is saved and updated after each interface crossing. This index is used to determine which velocity function must be used in the integration of the equations. A flag for each interface is also provided which indicates the decision to make in case the ray arrives at the interface. This allows one to model *P*- and *S*-waves, or even a conversion between the two, or to force a reflection at any given interface to simulate a reflector.

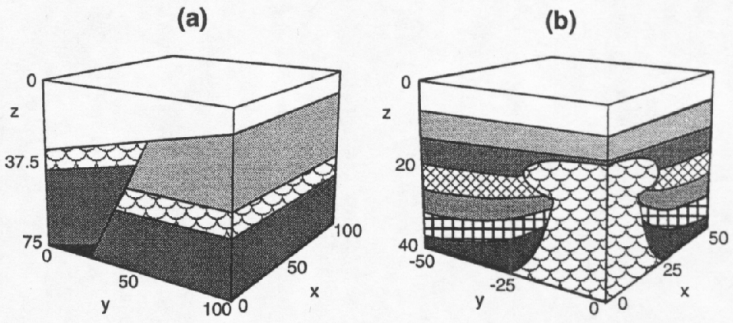

Figure 1: (a) Fault model. (b) Salt-dome model (partially shown).

BOUNDARY-VALUE PROBLEM (BVP)

The two-point ray tracing problem using SART is based on the straight-ray construction (Velis and Ulrych, 1996), and can be stated as follows. Both source, $\mathbf{x}_s$, and receiver, $\mathbf{x}_r$, are fixed and the optimum take-off angles θ_s and ξ_s are to be found so that the total traveltime is a global minimum (refer to Figure 2a). The total traveltime (cost function) is written as

$$\Phi(\theta_s, \xi_s) = \mathrm{T}_{se} + \mathrm{T}_{er}, \tag{1}$$

where T_{se} is the traveltime which is obtained after solving the IVP from the source to the point where the ray exits the model boundaries, $\mathbf{x}_e$. The second term, T_{er}, is the traveltime associated with the straight-ray construction. Since two angles are required to determine uniquely the whole ray trajectory, Φ is a two-dimensional function, and often multimodal and non-differentiable. When Φ is minimum, Fermat's principle is satisfied and $\mathbf{x}_e$ coincides with the receiver.

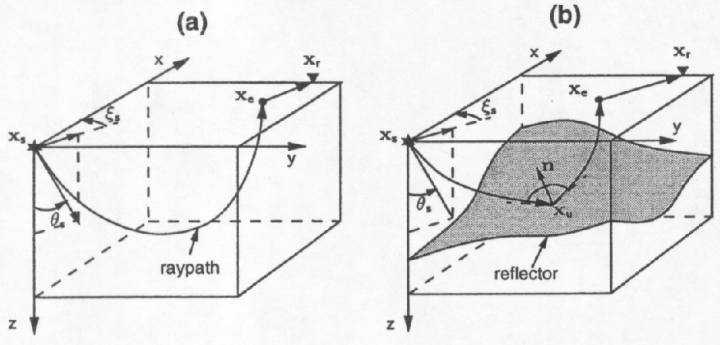

Figure 2: SART strategy for tracing (a) direct waves and (b) reflections.

The above procedure can be extended to deal with reflected waves (Figure 2b). Now we write the cost function

$$\Phi(\theta_s, \xi_s) = \begin{cases} \mathrm{T}_{su} + \mathrm{T}_{ue} + \mathrm{T}_{er} & \text{reflection=}\textit{true} \\ \mathrm{T}_{max} & \text{otherwise,} \end{cases} \tag{2}$$

where $\mathbf{x}_u$ is the point where the ray intersects the reflector, and T_{max} is the maximum guessed value T_{sr} may take for all possible take-off angles. As usual, the ray is propagated from the source with take-off angles θ_s and ξ_s until it arrives to the reflector at point $\mathbf{x}_u$. Here Snell's Law of reflection is applied and the propagation continues until the ray leaves the model boundaries at the emerging point $\mathbf{x}_e$. Finally, this point is connected with the receiver using a straight line. Similar strategies can be devised for tracing normal rays, headwaves and multiples (Velis, 1998).

SIMULATED ANNEALING OPTIMIZATION

We minimize the above cost functions using VFSA (Ingber, 1989), a very efficient stochastic method for solving hard nonlinear optimization problems. Take-off angle values are drawn from a Cauchy-like distribution that depends on a control temperature, which is gradually decreased. At high temperatures, the model space is sampled more or less uniformly. But at low temperatures, models with lowest cost function values are preferably sampled. Convergence is achieved at

Sixth International Congress of the Brazilian Geophysical Society

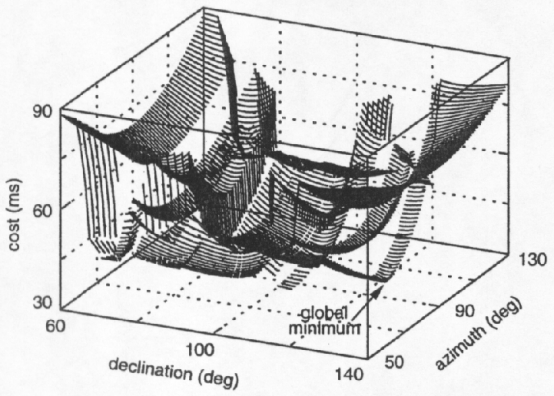

Figure 3: Traveltime vs take-off angles in the fault model.

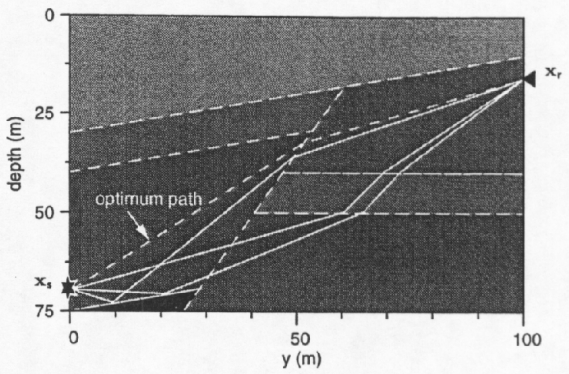

Figure 4: Multipathing in the fault model.

low temperatures when no further improvement in the cost function is observed. The advantage of VFSA over traditional SA techniques relies in the choice of the generating distribution and the cooling schedule. The long-tailed distribution permits exploration of the model space more effectively, and a faster cooling rate is allowed to accelerate convergence. Furthermore, the temperature associated with each parameter is adapted dynamically (*re-annealing*) according to the sensitivity of the cost function to each dimension in the model space.

Despite the fact that VFSA converges significantly faster than conventional SA methods, when Φ is close to the global minimum, taking T_{er} to zero may take several iterations. At these low temperature stages, SART switches to a local optimization algorithm to minimize the distance between the emerging and the receiver points. Locally, this is a well-behaved function, and the convergence to the global minimum is guaranteed. In practice a few iterations (two to eight) are enough to take T_{er} virtually to zero within machine precision.

NUMERICAL EXAMPLES

Model 1 is comprised of seven regions with constant velocities delimited by planar interfaces and a fault plane, as shown in Figure 1. We placed a source at $(50, 0, 70)$ and a receiver at $(50, 100, 16.5)$ and computed Φ vs θ_s and ξ_s (Figure 3). The nonlinearity of the cost function and the complexity of the optimization problem are evident.

What makes it difficult to globally minimize this function is not only the presence of local minima, but also the great number of discontinuities generated by the model. SA appears to be a natural tool for solving this kind of nonlinear optimization problems. While there are many possible solutions to the BVP, there is only one solution with a global minimum: $\Phi_{opt} = 34.714$ ms, $(\theta_s, \xi_s) = (125.90°, 90.00°)$. The other rays arriving to the receiver are local minima. These raypaths, together with the SART solution, are plotted in Figure 4.

Model 2 represents a salt dome with several layers and laterally varying velocities, as illustrated in Figure 1. For simplicity consider first a vertical slice of the model (the plane $x = 0$) and $\xi = 90°$ for all raypaths, so that they all lie on the same plane. We located a source at $(0, -50, 0)$ and produced a fan of 10,000 rays with equally spaced take-off angles in the range $[35°, 85°]$. Figure 5 shows Φ vs θ_s for a receiver located at $(0, 50, 0)$. The complexity of this function is enormous. It exhibits a large number of discontinuities and local minima, some of which correspond to solutions of the BVP. A detailed inspection of the curve reveals that the global minimum lies in a very narrow valley of only 0.1 degrees wide. If take-off angle ξ_s is also taken into account, the topography of $\Phi(\theta_s, \xi_s)$ becomes so complex we were not able to plot it, or even to generate it without missing too many features. Despite the rather difficult optimization problem, SART found the global minimum in about 500 iterations: $\Phi_{opt} = 39.735$ ms, $(\theta_s, \xi_s) = (54.40°, 90.00°)$. Figure 6a shows all the solutions to the BVP together with the optimum raypath obtained by SART.

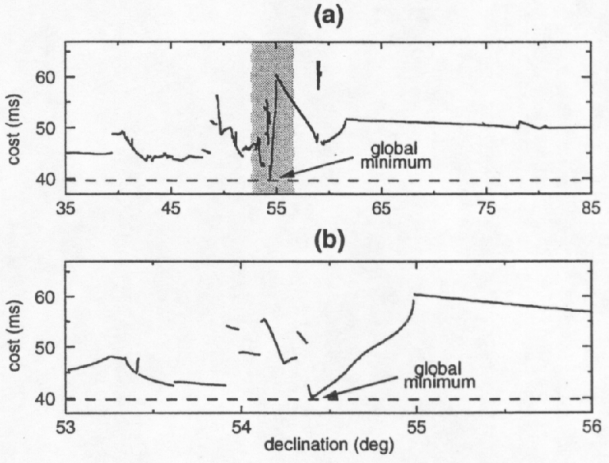

Figure 5: (a) Traveltime vs declination in the salt-dome model. (b) Blow out of the shaded region in (a).

Finally, we used SART to find all the raypaths connecting the same source and 41 different receivers uniformly distributed along the right borehole. The solutions are plotted in Figure 6b. Note that most of the trajectories are within one of two very

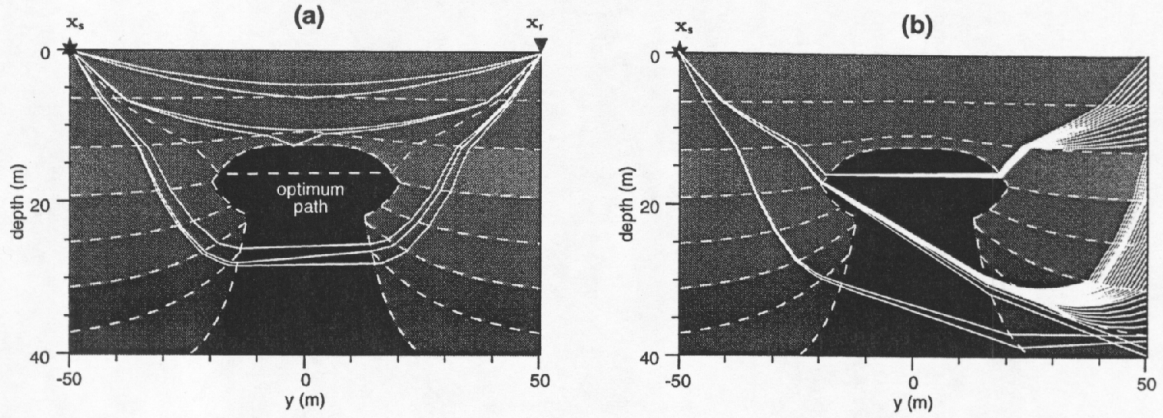

Figure 6: (a) Multipathing in the salt-dome model. (b) SART solutions for several receivers on the right borehole.

narrow take-off angle beans. This illustrates the difficulties that a ray-tracing method would have to face to find the desired solution.

CONCLUSIONS

SART is a very versatile computational algorithm for solving the boundary-value ray-tracing problem in general 2-D/3-D models. SART aims to find the raypath connecting any source-receiver pair so that the associated traveltime is a global minimum. The solution is found after solving iteratively a highly nonlinear optimization problem by means of VFSA. The results are independent of the initial guess, since VFSA is a global optimization algorithm. At each iteration, SART solves numerically the equations derived from the high-frequency ray approximation theory. This scheme is coupled with a versatile model parameterization system that allows one to represent a wide variety of geologic 3-D (or 2-D) structures. Any number of regions delimited by arbitrary interfaces can be defined. The velocity within each region is specified separately, which allows one to model any type of waves, including converted waves.

SART exhibits important improvements over existing ray-tracing techniques like bending and shooting. The problem of local minimum paths is eliminated provided enough iterations are performed. Despite the fact that SART solves an IVP at each iteration, the selection of the appropriate take-off angles does not represent a serious difficulty even for ill-behaved cost functions. An exhaustive numerical comparison between SART and conventional shooting techniques (not shown here for space reasons), demonstrates that SART is significantly faster for obtaining the desired solution for a given accuracy.

It is worthwhile mentioning that the optimum raypath obtained by SART corresponds to a particular solution of the IVP. Consequently, first-arrival raypaths traveling across shadow zones and arbitrary head-waves cannot, in general, be found. However, later arrivals like reflections, head-waves, and multiples can be obtained by specifying a ray signature in the way of constraints and writing down the appropriate cost function.

REFERENCES

Červený, V., 1987, Ray-tracing algorithms in three-dimensional laterally varying layered structures: in Seismic Tomography with applications in Global Seismology and Exploration Geophysics, E. Reidel, 99–133.

Fisher, R., and Lees, J.M., 1993, Shortest path ray tracing with sparse graphs: Geophysics, 58, 987–996.

Ingber, L., 1989, Very fast simulated re-annealing: Mathl. Comput. Modeling, 12, 967–973.

Moser, T., Nolet, G., Snieder, R., 1992, Ray bending revisited: Bull. Seis. Soc. Am., 82, 259–288.

Sambridge, M.S., and Kennett, B.L., 1990, Boundary-value ray tracing in a heterogeneous medium: a simple and versatile algorithm: Geophys. J. Int., 191, 157–168.

Velis, D.R., and Ulrych, T.J., 1996, Simulated annealing two-point ray tracing: Geophys. Res. Lett., 23, 201–204.

Velis, D.R., 1998, Application of simulated annealing to some seismic problems: PhD Thesis, University of British Columbia, Canada.

ACKNOWLEDGMENTS

We are grateful to M. Bostock and R. Pawlowicz for useful discussions and constructive comments. This research was partially funded by Consortium for the Development of Specialized Seismic Techniques (CDSST), University of British Columbia, Canada.